

Identification of Feeder Vessels in Ocular Surface Neoplasia using Indocyanine Green Angiography

A Preliminary Report

Authors: Matthias Brunner, MD^{1,2}, Bernhard Steger, MD³, Vito Romano, MD^{2,4}, Martin Hodson¹, Yalin Zheng, PhD⁴, Heinrich Heimann, MD, PhD¹, Stephen B. Kaye, MD, FRCOphth^{2,4}

Affiliations:

1. Liverpool Ocular Oncology Service, St. Paul's Eye Unit, Royal Liverpool University Hospital, Liverpool, United Kingdom
2. Department of Corneal and External Eye Diseases, St. Paul's Eye Unit, Royal Liverpool University Hospital, Liverpool, United Kingdom
3. Department of Ophthalmology, Medical University of Innsbruck, Innsbruck, Austria
4. Department of Eye and Vision Science, University of Liverpool, Liverpool, United Kingdom

Corresponding author:

Matthias Brunner
St. Paul's Eye Unit,
Royal Liverpool University Hospital,
8Z Link, Prescot Street, Liverpool, UK
L7 8XP
Phone: 0151 706 2134
Fax: 0151 706 5861
E-mail: matthias@brunnermail.ch

ABSTRACT

Purpose: To evaluate indocyanine green angiography (ICGA) for the identification and characterization of afferent (feeding) and efferent (draining) vessels in patients with ocular surface neoplasia.

Materials and Methods: Consecutive patients with biopsy-proven benign, pre-invasive or invasive ocular surface tumors of the bulbar conjunctiva were included. Patients underwent anterior segment optical coherence tomography, ICGA, and colour photography for the evaluation of the thickness, location, number and diameter of afferent and efferent vessels of the lesions.

Results: Twenty-two eyes of 22 patients with papillomas (n=4), intra-epithelial neoplasia lesion (n=2) in situ or invasive carcinomas (n=6), nevus (n=5), conjunctival melanocytic intra-epithelial neoplasia lesion (n=1), and in situ or invasive melanomas (n=4) were investigated. Afferent (feeder) vessels were identified in all lesions. There were fewer afferent (3.1 ± 1.6) than efferent (7.5 ± 3.5) vessels per lesion ($p < 0.001$) and the mean diameter was smaller for afferent ($101 \pm 62 \mu\text{m}$, 28-281) than efferent vessels ($137 \pm 51 \mu\text{m}$, 31-652; $p = 0.017$). The number of afferent and efferent vessels was associated with the thickness of the lesion ($p = 0.037$, $p < 0.01$). Lesion filling times differed between benign and invasive or pre-invasive lesions ($p = 0.018$).

Conclusions: ICGA is a useful adjunctive *in vivo* imaging method for the assessment of the vasculature in patients with suspected ocular surface neoplasia.

INTRODUCTION

Characterising the vasculature of neoplastic lesions is important in assessing tumour development, growth and response to treatment.(1) Pathological angiogenesis is a particular hallmark of solid neoplasia. Sufficient supply of oxygen and nutrients is critical for neoplastic cell proliferation and tumour survival.(2) While very small, early stage tumours may obtain their oxygen and nutrients by means of diffusion from surrounding tissue vessels, larger tumors that grow beyond a size of 2 mm³ can no longer be sustained by diffusion and require an internal blood supply.(3) The vasculature of tumours, however, is complex and vessel networks in tumours have unique features that differ fundamentally from those seen in normal vasculature. (4,5) These typically consist of a disorganized labyrinth of vessels which lack the conventional hierarchy of arterioles, capillaries and venules seen in normal vascular networks.(4) Tumour vessels are often tortuous with variable diameters, abnormal bulges and blind ends; sometimes accompanied by arteriolar-venous shunts and plasma channels lacking red blood cells.(6) The vessels are poorly invested with smooth muscle cells and may have a discontinuous endothelial cell lining with an abnormal basement membrane, resulting in increased vessel permeability.(7)

Several imaging methods such as magnetic resonance imaging (MR), computed tomography (CT), positron emission tomography, Doppler ultrasonography, and spectroscopy are used to evaluate vascular networks.(8) In the field of ophthalmology, fluorescein and indocyanine green angiography (FA and ICGA) are a very well established and widely used imaging method for the diagnosis and management of a variety of chorioretinal vascular diseases.(9,10) Anterior segment angiography can also be used to investigate the ocular surface vasculature and has gained growing popularity for the clinical assessment of a variety of corneal and extracorneal ocular surface diseases in recent years.(11,12) The better delineation of vessels compared to biomicroscopic assessment and the capability to identify the afferent and efferent vessels makes this imaging technique an invaluable tool for investigating morphological vessel characteristics and blood flow dynamics in vascularized lesions. (13-15) ICGA and FA in conjunction with objective computer-assisted image analysis

has been demonstrated to provide a reliable method for quantifying vessel change in corneal angiogenesis by measuring vessel parameters such as diameter, length, branch pattern and tortuosity.(13) Leakage of fluorescein using FA may reflect vessel maturity and offer the potential to functionally stage angiogenesis.(16)

In contrast to choroidal and retinal lesions, vessel characteristics and haemodynamics in ocular surface tumours are still poorly understood and the clinical and prognostic role of tumour-feeding (afferent) and draining (efferent) vessels remains unknown. In this study we evaluated the use of indocyanine green angiography to identify and assess afferent and efferent vessels in patients with benign and malignant neoplastic lesions of the ocular surface.

MATERIALS AND METHODS

Patients referred to the Liverpool Ocular Oncology Service between March and October 2016 with clinically evident pigmented and non-pigmented tumours of the limbal and extra-limbal bulbar conjunctiva were prospectively recruited. All participants had a detailed slit-lamp biomicroscopy and underwent subsequent anterior segment imaging including colour photography, AS-OCT and indocyanine green angiography during the same visit. Patient demographics (age, gender, ethnicity) and clinical tumour characteristics (size, thickness, location, limbal involvement, pigmentation) were collected using a standardised data collection sheet. Tumours with diffuse margins or indiscernible vessels and tumours with non-bulbar conjunctival location were excluded. All patients underwent excisional or incisional biopsy for histopathology. All specimens were assessed by an experienced pathologist at the pathology department of our institution. For pre-invasive melanocytic neoplasia, the term conjunctival melanocytic intra-epithelial neoplasia (C-MIN) was used (also referred to as PAM with atypia), and the severity of dysplasia was graded using the histopathological classification system (score 1-10) of Damato and Coupland.⁽¹⁷⁾ None of the patients had had previous treatment for their ocular surface tumours. Informed consent was obtained from all subjects and the study was approved by the Institutional Review Board and adhered to the Tenets of the Declaration of Helsinki.

Colour images

Colour images were recorded using a slit lamp mounted digital system (SL-D Digital Slit Lamp; Topcon, Tokyo, Japan) as per our existing protocol for standardised colour images: The entire ocular surface was imaged in all 9 positions of gaze using a 10x to 25x magnification and illumination from a 45 degree angled beam on slit lamp biomicroscopy with a diffuser filter and a variable flash intensity. A total of 18 color images (9 images per eye) were obtained for each patient.

Anterior-segment optical coherence tomography

Anterior segment OCT was performed with an OCT lens in conjunction with the HRA2 Scanning Laser Ophthalmoscope (Heidelberg Engineering, Heidelberg, Germany) for thickness measurements of tumours. Cross sectional scans at an angle of 0 and 90 degrees were obtained for every lesion and the measurements were taken at the thickest tumour location.

Indocyanine Green Angiography

An HRA2 Scanning Laser Ophthalmoscope (*Heidelberg Engineering, Heidelberg, Germany*) with a 20° imaging lens and a focus setting of +32.00D was used for ICGA as previously described.(13,14,16) After intravenous injection of 5ml of 5mg/ml indocyanine green dye (Pulsion Medical Systems, Munich, Germany) into a peripheral arm vein, videography was undertaken for 30 to 60 seconds concentrating on the region of interest (ROI), commencing when the dye fluoresced within the eyelids, usually approximately 10 seconds after the injection (depending on age of the patient and the location of the ROI).(16) Following videography, single-frame ICGA photographs of the ROI including the tumour and surrounding blood vessel fluorescence were captured at a 32 to 34x magnification every 3 to 5 seconds for 3 minutes in high-resolution mode incorporating automatic real-time (ART) software.

Image analysis

ICGA video frames were used to identify the afferent (feeding) and efferent (draining) vessels of each lesion. Afferent vessels were defined as those vessels in which the dye first appeared with anterograde filling towards the tumour. Efferent vessels were defined as vessels filling in a retrograde fashion away from the tumor during or with a latency to intralesional vessel filling. Lesion filling time was defined as the time interval (in seconds) between first dye appearance in afferent and first dye appearance in efferent tumour vessels. The ICGA images were graded using a subjective quality score of 0 to 4 as previously described (0, no vessel discernible; 1, poor vessel delineation; 2, good vessel delineation; 3,

very good vessel delineation; 4, excellent vessel delineation).(13) The two best-quality frames demonstrating, first filling of afferent vessels and then complete filling of efferent vessels were independently assessed by two observers (M.B. and V.R.). The two best-quality frames with complete afferent and efferent vessel filling of the ROI were then selected by the same two observers for calculation of vessel diameters. This was performed using an in-house automated program written in numerical computing language (Matlab R14; The Mathworks Inc., Natick, MA) as described and validated elsewhere.(13) Briefly, the software can detect vessels and extract quantitative information of the detected vasculature by performing a series of image processing tasks mainly including image enhancement, enhancement of vessel structures and conversion to binary images. The pixel resolution (mm/pixel) of the angiographic images, defined as the ratio between the diameter of the cornea (12 mm) and the image diameter of the tumour (or two set landmarks within the lesion) in pixels, was estimated by identifying the limbus to limbus diameter manually and calculation of the pixels number within these landmarks. The vessel diameters were measured within a distance of 0.5 to 1 mm from the tumour margin. The orientation of tumour vessels was categorized as the “same”, if the entry and exit points of afferent and efferent vessels at the tumour margin were located less than 90 degrees apart, and as ‘opposite’, if these were located more than 90 degrees apart.

Statistical analysis

Data were expressed as means \pm SD. The Shapiro-Wilk test was used to test for non-normal distribution of the data. The Mann-Whitney U test was used to compare vessel number, diameter and lesion filling times. P values of less than 0.05 were considered statistically significant. Levels of agreement were tested using Fleiss' Kappa Statistic (k). Interpretation of levels of agreement were based on that described for two (binary) categories for each patient. A value of <0.2 , k was considered slight, $0.2 < k < 0.4$ fair; $0.4 < k < 0.6$ moderate, $0.6 < k < 0.8$ substantial and $k > 0.8$ as almost perfect. Statistical analyses were performed

with the Statistical Package for the Social Sciences Software (IBM SPSS Version 22.0 for MAC; SPSS Inc., Chicago, IL).

RESULTS

Twenty-two eyes of 22 patients (median, 68 years; range, 23-88 years; female-to-male ratio, 6:16) with ocular surface neoplasia of the bulbar conjunctiva were included. The demographic patient data and clinical tumour characteristics are included in *Table 1*. The majority of patients were caucasians (n=16). The examined tumours included 12 squamous lesions (4 papillomas, 2 intra-epithelial neoplasia lesions (CIN 2), 5 in situ carcinomas (CIN 3), 1 invasive carcinoma, SCC), and 10 melanocytic lesions (5 naevi, 1 melanocytic intra-epithelial neoplasia lesion (C-MIN score 3), 1 melanoma in situ, and 3 invasive melanomas). The temporal bulbar conjunctiva was the most common site of involvement (n=11) and the majority of lesions involved the limbus (n=14) with or without corneal extension. Eleven lesions presented with intrinsic pigmentation. The mean largest basal diameter and maximum tumour thickness measured 8.3 ± 3.5 mm (range, 3-16) and 724 ± 299 μ m (range, 346-1217), respectively. All eyes underwent complete excision (n=20) or incisional biopsy (n=2) and histopathological diagnosis was confirmed in all cases (*Table 1*).

Inter-observer agreement for grading the quality of image assessment and was substantial for the selected ICGA frames ($k=0.72$; $p<0.01$) and excellent for afferent and efferent vessel identification ($k=0.88$; $p<0.01$). The vessel parameters are summarized in *Table 2*. A mean of 3.1 ± 1.6 (range, 1-7) afferent and 7.5 ± 3.5 (range, 2-14) efferent vessels were found per lesion ($p<0.001$). The ratio of the number of afferent to efferent vessels was 0.49 ± 0.28 (range, 0.17-1.25). Afferent and efferent vessel diameters ranged from 28 to 281 μ m (mean, 101; SD ± 51) and 31 to 652 μ m (mean, 136; SD, ± 62), respectively ($p=0.2$) with a ratio of 0.80 ± 0.35 (range, 0.7-1.6).

Afferent and efferent vessel number and diameter varied among the different patient subgroups (*Table 3, supplementary data*), but did not differ significantly between squamous and melanocytic lesions, or between benign and pre-invasive or invasive lesions. There were significant associations between the number of afferent ($R^2=0.59$, $p=0.037$), and efferent ($p<0.01$) vessels, vessel diameter ($R^2=0.35$, $P=0.05$) and tumour thickness, but not with the size (largest basal diameter) of the lesion. Intralesional filling times were significantly longer

in benign (3.19 ± 2.20 sec) than pre-invasive (2.49 ± 1.10 sec) or invasive lesions (1.95 ± 0.81 sec) ($p=0.018$), and were also dependent on the location of vessel entry and exit points at the tumour margins ($p=0.001$).

In two patients with papillomas, the conformation of the afferent vessels was more coiled relative to the accompanying efferent vessels, as demonstrated in *Figure 1A-C*. In some neoplasms, afferent vessels accompanied efferent vessels, biomicroscopically presenting as finer vessels aligning the efferent vessels in a parallel fashion (*Figures 2A-C*). In other lesions, afferent vessels were not located in close proximity to efferent vessels (*Figures 3A-C*). The discord between afferent and efferent vessel diameters was most noticeable in papillomas, as these lesions presented with relatively small afferent and larger-diameter efferent vessels compared to other lesions. Of note, none of the afferent vessels in the examined lesions showed the increased tortuosity as commonly seen in efferent vessels.

DISCUSSION

The architecture and haemodynamics of vascular networks has been investigated in various extraocular tumours.(4,5,18) To the best of our knowledge, this is the first study to report the use indocyanine green angiography (ICGA) for identification and evaluation of afferent and efferent vessel parameters in various ocular surface tumors including benign, pre-invasive and invasive lesions. The use of ICGA for the evaluation and treatment of corneal neovascularization has been well documented. (13,14,16) ICGA has been shown to provide excellent vessel delineation and to differentiate afferent and efferent vessels in neovascular corneal networks and in allergic eye disease.(13,14,16,19,20) In this study, the systematic analysis of videoangiography frames enabled us to evaluate the dye appearance dynamics of vascular networks in each lesion. This allowed for consistent identification of afferent vessels, possibly representing tumour-feeding arteries, and their efferent counterparts, presumably representing draining veins. Using the angiographic images it was possible to differentiate afferent and efferent vessels on biomicroscopy and in colour images. Similar to the good imaging of corneal neovascularisation in the presence of scars or exudate, imaging of the tumour vasulature with ICGA was obtained regardless of the thickness of the lesion. This is important as the vasculature of thicker lesions is very difficult to discern with colour photography. Unlike fluorescein, indocyanine green does not show vessel leakage in early filling phases, and as such is more suitable for fluorescence angiographic vessel delineation in ocular surface lesions.

The term 'feeder vessel' is widely used to describe clinical features of ocular surface tumours and usually refers to prominent tumor vessels seen on biomicroscopy. None of the tumour vessels with prominent appearance on colour images represented afferent i.e true feeder vessels in our case series. Our findings would suggest that this terminology may represent a misnomer in a considerable proportion of cases, as it may be impossible to accurately identify the true afferent and efferent tumour vessels based on biomicroscopy or colour images alone. We would therefore suggest that the terms feeder and drainer vessels only be used if confirmed with angiography or other imaging modes which provide 'direction of flow'

information. The presence of feeder vessels has been considered to represent a possible risk factor for malignancy in different studies.(21,22) When interpreting these data it has to be considered that the presumed feeder vessels in these studies were based solely on biomicroscopic findings and may have included afferent and efferent vessels or perhaps efferent vessels only.

The identification of afferent tumour vessels using fluorescence angiography may also have potential clinical implications for the pre- and peri-operative management of ocular surface neoplasia. Interestingly, we observed a significant association of lesional vessel filling times and the tumour dignity, with longer filling times in benign than in pre-invasive or invasive lesions. We hypothesize that these findings may indirectly reflect haemodynamic changes caused by the structural vascular heterogeneity in tumours, which may vary with the severity of disease i.e grade of dysplasia. Increased structural heterogeneity of vascular networks is a well-known feature of neoplastic lesions(5) Vascular networks of tumours contain tortuous vessels, shunts, vascular loops, widely variable intervascular distances, and large avascular areas(1,4,18), and regions of stagnant or intermittent blood flow within these networks have been observed.(23,24) Functional shunts within vascular networks of induced squamous carcinoma in a mouse model have been demonstrated using intravital microscopy(5). Increased (functional) shunting may also explain the different filling times observed for the tumours in our cohort, and as such, may have the potential to be used as diagnostic biomarkers for the severity of disease in ocular surface neoplasia.

Angiographically guided identification and selective fine needle diathermy (FND) to the afferent (feeder) vessels has been shown to minimise the amount of diathermy needed to be effective in treating corneal neovascularisation.(14) Preoperative selective occlusion of afferent vessels with FND(14,25) may therefore reduce intraoperative bleeding during tumour excisions and reduce the risk of potential tumour seeding in invasive melanomas. Shutting down the blood supply may in addition cause necrosis-induced tumour involution, thereby facilitating the surgical management of extensive mass lesions and contributing to the eradication of the tumour.

There are several limitations to this study. The case numbers were small with lesion heterogeneity (diagnosis, size and duration), and in particular there was selection bias; only including nodular ocular surface lesions with well-defined tumour margins. Patients with very extensive or diffuse lesions, and lesions involving the fornix or palpebral conjunctiva, were not investigated as such lesions are difficult to approach angiographically. Furthermore, only a small proportion of patients presenting with OSN were willing to undergo additional examinations including fluorescence angiography for study purposes. Due to the small number of patients with different types of neoplasia we may not have been able to detect differences in afferent and efferent vessel number and diameter between lesion type.

Despite these limitations we found ICGA to be a useful imaging method for the assessment of the vasculature in patients with suspected ocular surface neoplasia arising from the bulbar conjunctiva. Angiography enables accurate identification and localisation of afferent and efferent vessels and their respective characteristics. As in lesions elsewhere in the body, these vascular parameters may be of help in the assessment and management of patients with benign and malignant neoplastic lesions of the ocular surface.

Funding: None

Declaration of Interests: The authors report no conflicts of interest. The authors alone are responsible for the content and writing of the paper.

REFERENCES

1. Baish JW, Gazit Y, Berk DA, Nozue M, Baxter LT, Jain RK. Role of tumor vascular architecture in nutrient and drug delivery: an invasion percolation-based network model. *Microvasc Res*. 1996 May;51(3):327–46.
2. Carmeliet P, Jain RK. Angiogenesis in cancer and other diseases. *Nature*. 2000 Sep 14;407(6801):249–57.
3. Folkman J. Tumor angiogenesis: therapeutic implications. *N Engl J Med*. 1971 Nov 18;285(21):1182–6.
4. Konerding MA, Fait E, Gaumann A. 3D microvascular architecture of pre-cancerous lesions and invasive carcinomas of the colon. *Br J Cancer*. 2001 May 18;84(10):1354–62.
5. Pries AR, Cornelissen AJM, Sloot AA, Hinkeldey M, Dreher MR, Höpfner M, et al. Structural adaptation and heterogeneity of normal and tumor microvascular networks. *PLoS Comput Biol*. Public Library of Science; 2009 May;5(5):e1000394.
6. McDonald DM, Choyke PL. Imaging of angiogenesis: from microscope to clinic. *Nat Med*. 2003 Jun;9(6):713–25.
7. Gee MS, Procopio WN, Makonnen S, Feldman MD, Yeilding NM, Lee WMF. Tumor vessel development and maturation impose limits on the effectiveness of anti-vascular therapy. *AJPA*. 2003 Jan;162(1):183–93.
8. van Vliet M, van Dijke CF, Wielopolski PA, Hagen ten TLM, Veenland JF, Preda A, et al. MR angiography of tumor-related vasculature: from the clinic to the micro-environment. *Radiographics*. 2005 Oct;25 Suppl 1(suppl_1):S85–97–discussionS97–8.
9. Brancato R, Trabucchi G. Fluorescein and Indocyanine Green Angiography in Vascular Chorioretinal Diseases. *Semin Ophthalmol*. Taylor & Francis; 2009 Jul 2;13(4):189–98.
10. Stanga PE, Lim JI, Hamilton P. Indocyanine green angiography in chorioretinal diseases: indications and interpretation: an evidence-based update. *Ophthalmology*. 2003 Jan;110(1):15–21–quiz22–3.

11. Easty DL, Bron AJ. Fluorescein angiography of the anterior segment. Its value in corneal disease. *British Journal of Ophthalmology*. BMJ Group; 1971 Oct;55(10):671–82.
12. Nieuwenhuizen J, Watson PG, Emmanouilidis-van der Spek K, Keunen JEE, Jager MJ. The value of combining anterior segment fluorescein angiography with indocyanine green angiography in scleral inflammation. *Ophthalmology*. 2003 Aug;110(8):1653–66.
13. Anijeet DR, Zheng Y, Tey A, Hodson M, Sueke H, Kaye SB. Imaging and evaluation of corneal vascularization using fluorescein and indocyanine green angiography. *Investigative Ophthalmology & Visual Science*. 2012 Feb;53(2):650–8.
14. Spiteri N, Romano V, Zheng Y, Yadav S, Dwivedi R, Chen J, et al. Corneal Angiography for Guiding and Evaluating Fine-Needle Diathermy Treatment of Corneal Neovascularization. *Ophthalmology*. 2015 Apr 1;122(6):1079–84.
15. Romano V, Steger B, Zheng Y, Ahmad S, Willoughby CE, Kaye SB. Angiographic and In Vivo Confocal Microscopic Characterization of Human Corneal Blood and Presumed Lymphatic Neovascularization: A Pilot Study. *Cornea*. 2015 Nov;34(11):1459–65.
16. Kirwan RP, Zheng Y, Tey A, Anijeet D, Sueke H, Kaye SB. Quantifying changes in corneal neovascularization using fluorescein and indocyanine green angiography. *Am J Ophthalmol*. 2012 Nov;154(5):850–2.
17. Damato B, Coupland SE. Conjunctival melanoma and melanosis: a reappraisal of terminology, classification and staging. *Clin Experiment Ophthalmol*. Blackwell Publishing Asia; 2008 Nov;36(8):786–95.
18. Less JR, Skalak TC, Sevic EM, Jain RK. Microvascular architecture in a mammary carcinoma: branching patterns and vessel dimensions. *Cancer Res*. 1991 Jan 1;51(1):265–73.
19. Steger B, Romano V, Kaye SB. Angiographic Evaluation of Inflammation in Atopic Keratoconjunctivitis. *Ocul Immunol Inflamm*. 2016 Nov 30;:1–4.
20. Steger B, Romano V, Kaye SB. Corneal Indocyanine Green Angiography to Guide

- Medical and Surgical Management of Corneal Neovascularization. *Cornea*. 2016 Jan;35(1):41–5.
21. Gichuhi S, Macharia E, Kabiru J, Zindamoyen AM, Rono H, Ollando E, et al. Clinical Presentation of Ocular Surface Squamous Neoplasia in Kenya. *JAMA Ophthalmol*. American Medical Association; 2015 Nov;133(11):1305–13.
 22. Shields CL, Alset AE, Boal NS, Casey MG, Knapp AN, Sugarman JA, et al. Conjunctival Tumors in 5002 Cases. Comparative Analysis of Benign versus Malignant Counterparts. The 2016 James D. Allen Lecture. *Am J Ophthalmol*. 2016 Oct.
 23. Chaplin DJ, Hill SA, Bell KM, Tozer GM. Modification of tumor blood flow: Current status and future directions. *Seminars in Radiation Oncology*. 1998 Jul;8(3):151–63.
 24. Eskey CJ, Koretsky AP, Domach MM, Jain RK. 2H-nuclear magnetic resonance imaging of tumor blood flow: spatial and temporal heterogeneity in a tissue-isolated mammary adenocarcinoma. *Cancer Res*. 1992 Nov 1;52(21):6010–9.
 25. Romano V, Steger B, Brunner M, Ahmad S, Willoughby CE, Kaye SB. Method for Angiographically Guided Fine-Needle Diathermy in the Treatment of Corneal Neovascularization. *Cornea*. 2016 Jul;35(7):1029–32.

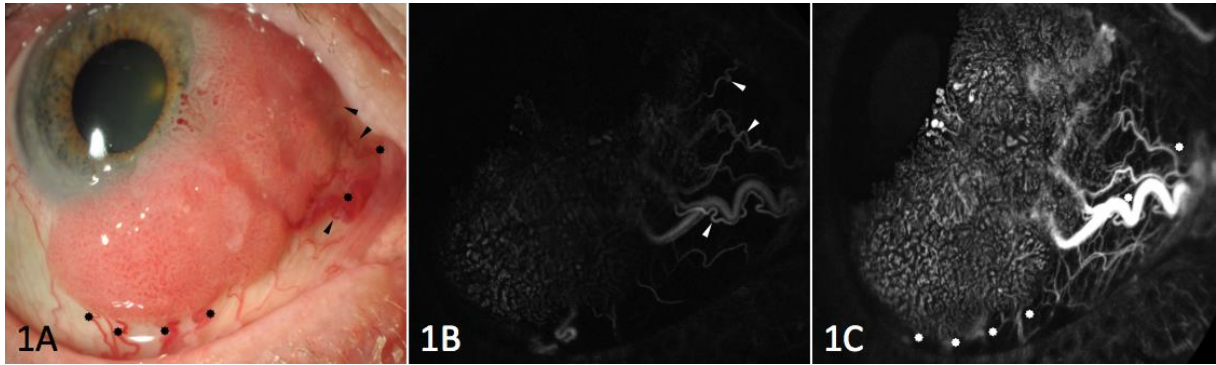


Figure 1. A, Slit-lamp photograph of a 97-year-old male patient showing a conjunctival papilloma, with afferent (black arrows) and efferent (black points) tumor vessels. B, Angiographic image of same eye (ICGA, 0:21:64 sec) showing afferent vessels (white arrows). C, Angiographic image of same eye showing (ICGA, 0:32:86 sec) efferent vessels (white points).

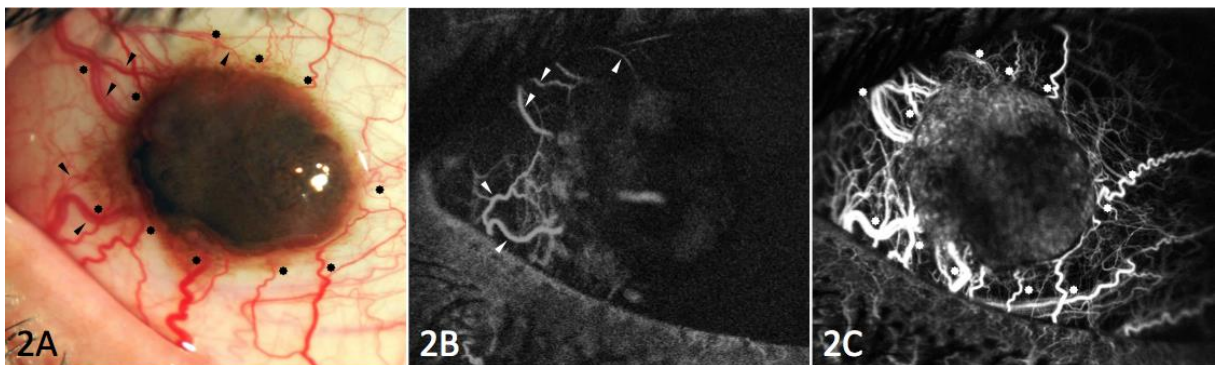


Figure 2. A, Slit-lamp photograph of a 29-year-old male patient showing conjunctival invasive melanoma, with afferent (black arrows) and efferent (black points) tumor vessels. B, Angiographic image of same eye (ICGA, 0:12:37 sec) showing afferent vessels (white arrows). C, Angiographic image of same eye showing (ICGA, 0:29:35 sec) efferent "drainier" vessels (white points).

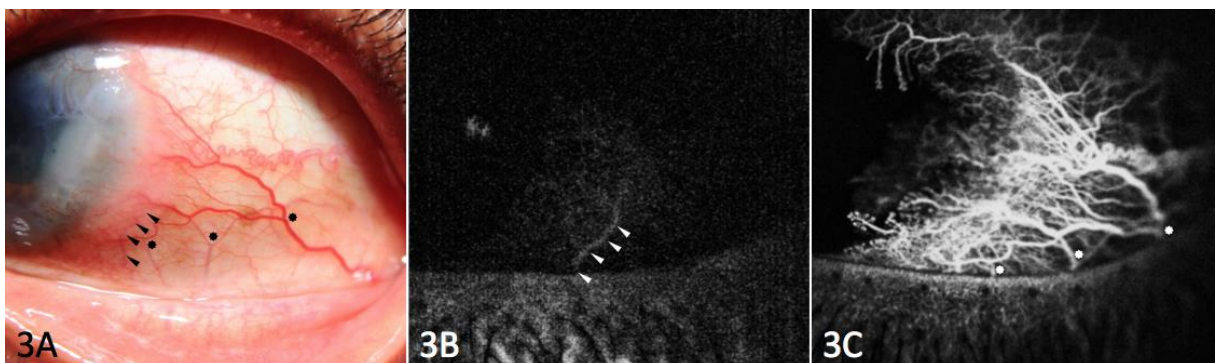


Figure 3. A, Slit-lamp photograph of a 55-year-old male patient showing conjunctival and

corneal intraepithelial neoplasia (CIN 2), with afferent (black arrows) and efferent (black points) tumor vessels. B, Angiographic image of same eye (ICGA, 0:10:28 sec) showing afferent vessels (white arrows). C, Angiographic image of same eye showing (ICGA, 0:17:86 sec) efferent vessels (white points).

Table 1. Patient Demographics and Clinical Tumour Characteristics

Patient No. (Gender, Laterality)	Age (Years)	Ethnicity	Histopathological Diagnosis*	Location (Bulbar Quadrant)	Limbal Involvement	Intrinsic Pigmentation	Largest Tumour Diameter [mm]	Tumour Thickness [μ m]
1 (M, OD)	79	Caucasian	Papilloma	Temporal, inferior	yes	no	16.0	980
2 (M, OD)	59	Caucasian	Papilloma	Inferior	no	no	5.1	457
3 (F, OS)	58	Caucasian	Papilloma	Inferior	no	no	10.6	1173
4 (M, OS)	80	Caucasian	Papilloma	Temporal	yes	no	6.7	556
5 (M, OS)	55	African	CIN 2	Temporal, inferior	yes	yes	11.5	549
6 (M, OD)	72	Caucasian	CIN 2	Nasal	yes	no	5.5	1107
7 (M, OS)	64	Caucasian	CIN 3 (CIS)	Temporal	no	no	5.5	673
8 (M, OD)	82	Indian	CIN 3 (CIS)	Temporal	yes	no	8.5	389
9 (F, OS)	86	Caucasian	CIN 3 (CIS)	Nasal, superior	yes	no	10.0	1217
10 (M, OD)	81	Caucasian	CIN 3 (CIS)	Nasal	yes	no	8.0	517
11 (M, OD)	82	Caucasian	CIN 3 (CIS)	Inferior, nasal,	yes	no	11.5	417
12 (M, OS)	75	Caucasian	SCC	Nasal	yes	no	5.8	1160
13 (F, OS)	77	Caucasian	Naevus	Nasal	no	yes	3.7	407
14 (F, OS)	33	Caucasian	Naevus	Nasal	no	yes	11.0	1042
15 (F, OD)	31	Caucasian	Naevus	Superior, temporal	yes	yes	3.0	448
16 (M, OS)	37	Middle-Eastern	Naevus	Temporal	yes	yes	4.9	579
17 (M, OD)	23	Middle-Eastern	Naevus	Temporal	no	yes	9.4	585
18 (F, OD)	63	Hispanic	C-MIN (Score 3) [†]	Temporal	yes	yes	4.6	346
19 (M, OS)	75	Caucasian	Melanoma in situ	Inferior, nasal	yes	yes	15.1	588
20 (M, OS)	88	Caucasian	Melanoma	Temporal, inferior	yes	yes	10.4	731
21 (M, OD)	29	Middle-Eastern	Melanoma	Temporal	no	yes	6.5	923
22 (M, OD)	56	Caucasian	Melanoma	Nasal	no	yes	10.0	1090
Mean	63.0						8.3	724
± SD	20.5						3.5	299
Min-Max	23-88						3.0-16.0	346-1217

F=female; M=male; OD=right eye; OS=left eye; CIN=conjunctival/corneal intraepithelial neoplasia; C-MIN=conjunctival/corneal melanocytic intraepithelial neoplasia; CIS=squamous cell carcinoma in situ; SCC=invasive squamous cell carcinoma.

*All patients underwent excisional (n=20) or incisional biopsy (n=2).

[†]Classification of C-MIN based on scoring systems (0-10) by Damato and Coupland.

Table 2. Angiographic Parameters of Afferent and Efferent Tumour Vessels

Patient No.	Vessel No.			Mean Vessel Diameters (\pm SD, min-max) [μ m]			Intralesional vessel filling [sec] [†]
	Afferent	Efferent	Ratio*	Afferent	Efferent	Ratio*	
1	3	12	0.25	98 (\pm 24, 72-117)	212 (\pm 156, 110-644)	0.46	0.84
2	2	2	1.00	95 (\pm 0, 0)	164 (\pm 43, 133-195)	0.58	8.41
3	4	11	0.36	174 (\pm 76, 101-281)	208 (\pm 125, 87-520)	0.84	2.95
4	2	8	0.25	158 (\pm 96, 90-226)	179 (\pm 63, 83-263)	0.88	3.81
5	1	3	0.33	121 (\pm 0, 0)	109 (\pm 18, 95-129)	1.11	0.97
6	3	7	0.43	46 (\pm 13, 32-58)	65 (\pm 17, 51-99)	0.71	1.47
7	3	9	0.33	115 (\pm 48, 70-166)	135 (\pm 36, 87-202)	0.85	3.67
8	2	2	1.00	241 (\pm 22, 226-256)	190 (\pm 4, 188-193)	1.27	2.32
9	4	10	0.40	60 (\pm 8, 51-70)	88 (\pm 37, 47-167)	0.68	2.93
10	1	5	0.20	64 (\pm 0, 0)	82 (\pm 14, 70-104)	0.78	2.2
11	3	14	0.21	38 (\pm 15, 28-49)	144 (\pm 34, 102-192)	0.26	1.37
12	3	7	0.43	42 (\pm 6, 36-48)	115 (\pm 69, 62-257)	0.37	1.06
13	3	6	0.50	55 (\pm 16, 43-73)	102 (\pm 23, 80-144)	0.54	3.42
14	3	6	0.50	40 (\pm 12, 30-54)	130 (\pm 56, 89-222)	0.31	2.54
15	3	7	0.43	69 (\pm 26, 44-95)	69 (\pm 17, 52-90)	1.00	1.27
16	5	4	1.25	107 (\pm 52, 62-192)	85 (\pm 13, 75-103)	1.26	3.5
17	3	4	0.75	108 (\pm 27, 91-140)	136 (\pm 24, 101-157)	0.79	2
18	3	7	0.43	94 (\pm 26, 69-121)	81 (\pm 39, 41-138)	1.16	3.5
19	7	10	0.70	103 (\pm 20, 74-125)	101 (\pm 16, 82-122)	1.02	4
20	2	12	0.17	164 (\pm 71, 113-214)	103 (\pm 30, 31-180)	1.59	2.5
21	7	13	0.54	146 (\pm 45, 86-208)	178 (\pm 98, 72-372)	0.82	1.48
22	2	6	0.33	91 (\pm 16, 79-102)	332 (\pm 197, 159-652)	0.27	2.75
Mean	3.1	7.5	0.49	101.32	136.73	0.80	2.68
\pm SD	1.6	3.5	0.28	51.38	62.41	0.35	1.62
Min-Max	1-7	2-14	0.17-1.25	38-241	65-332	0.26-1.59	0.84-8.41

*Afferent to efferent vessels.

[†]Defined as time period between first dye appearance in afferent and first dye appearance in efferent vessels (in seconds).

Supplementary data

Table 3. Subgroup Comparison of Afferent and Efferent Tumour Vessel Parameters

Subgroups (n)	Mean No. of Vessels (\pm SD, Min-Max)			Mean Vessel Diameters (\pm SD, Min-Max) [μ m]		
	Afferent	Efferent	Ratio*	Afferent	Efferent	Ratio*
Cell type						
<i>Melanocytic (10)</i>	3.8 (\pm 1.9, 2-7)	7.5 (\pm 3.1, 4-13)	0.56 (\pm 0.29, 0.17-1.25)	98 (\pm 38, 40-164)	132 (\pm 77, 69-332)	0.88 (\pm 0.41, 0.27-1.59)
<i>Squamous (12)</i>	2.6 (\pm 1.0, 1-4)	7.5 (\pm 4.0, 2-14)	0.43 (\pm 0.27, 0.20-1.00)	104 (\pm 62, 38-241)	141 (\pm 50, 65-212)	0.73 (\pm 0.29, 0.26-1.27)
<i>P-value</i>	0.1	0.8	0.09	0.9	0.2	0.3
Classification						
<i>Benign (9)</i>	3.1 (\pm 0.9, 2-5)	6.7 (\pm 3.3, 2-12)	0.58 (\pm 0.34, 0.25-1.25)	100 (\pm 44, 40-174)	143 (\pm 52, 69-212)	0.74 (\pm 0.30, 0.31-1.26)
<i>Pre-invasive or invasive (13)</i>	3.2 (\pm 1.9, 1-7)	8.1 (\pm 3.7, 2-14)	0.42 (\pm 0.22, 0.17-1.00)	102 (\pm 58, 38-241)	133 (\pm 71, 65-332)	0.84 (\pm 0.39, 0.26-1.59)
<i>P-value</i>	0.5	0.3	0.1	0.8	0.4	0.6
Location						
<i>Limbal (14)</i>	3 (\pm 1.6, 1-7)	7.8 (\pm 3.6, 2-14)	0.46 (\pm 0.32, 0.17-1.25)	100 (\pm 57, 38-241)	116 (\pm 47, 65-212)	0.89 (\pm 0.38, 0.26-1.59)
<i>Extra-limbal (8)</i>	3.4 (\pm 1.6, 2-7)	7.1 (\pm 3.6, 2-13)	0.53 (\pm 0.23, 0.33-1.00)	103 (\pm 44, 40-174)	173 (\pm 72, 102-332)	0.63 (\pm 0.24, 0.27-0.85)
<i>P-value</i>	0.5	0.5	0.2	0.7	0.04	0.1
Vessel orientation						
<i>Same (14)</i>	3.5 (\pm 1.7, 1-7)	7.9 (\pm 4.0, 2-14)	0.53 (\pm 0.30, 0.17-1.25)	106 (\pm 60, 38-241)	134 (\pm 46, 65-212)	0.81 (\pm 0.40, 0.26-1.59)
<i>Opposite (8)</i>	2.5 (\pm 0.9, 1-4)	6.8 (\pm 2.5, 2-10)	0.42 (\pm 0.25, 0.20-1.00)	93 (\pm 32, 60-158)	141 (\pm 88, 69-332)	0.78 (\pm 0.27, 0.27-1.16)
<i>P-value</i>	0.1	0.5	0.2	0.6	0.5	0.9

*Afferent to efferent vessels

†Location of entry and exit points of afferent and efferent vessels at tumour margin (same=within 90 degrees; opposite=more than 90 degrees apart).